Med Ultrason 2025, Vol. 27, no. 2, 240-252

Left atrial mass detected by cardiac ultrasonography – myxoma or something else?

Mijo Meter

Cardiovascular Diseases Department, University Hospital of Split, 21000 Split, Croatia

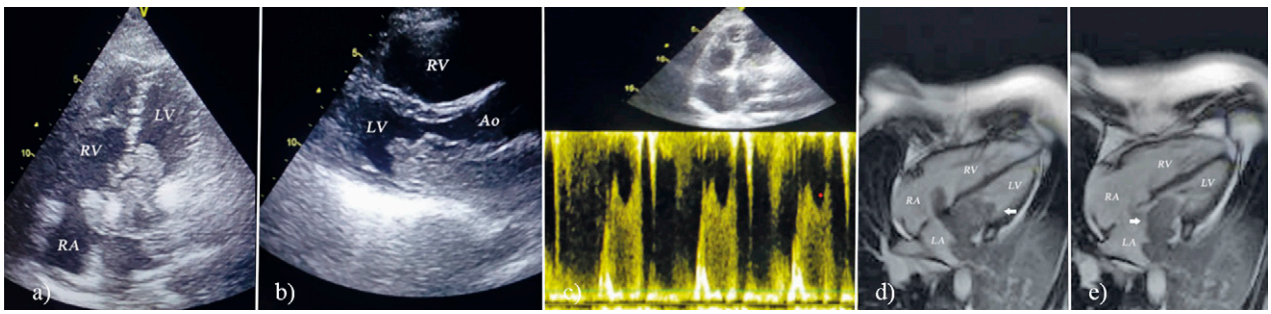

Fig 1. a) TTE showing left atrial mass prolapsing across the mitral valve; b) PLAX view revealing mass in the LA; c) Pulse wave Doppler showing increased gradient across the mitral valve; d) and e) cardiac MRI scan demonstrating a left atrial tumor (white arrow) prolapsing into the LV cavity and RA through the atrial septal defect. LA – left atrium, LV – left ventricle, RA – right atrium, RV – right ventricle, Ao – aorta

To the Editor,

A 48-year-old female patient with a history of previously resected inguinal synovial sarcoma presented to the emergency department with symptoms of cough, progressive dyspnoea and hemoptysis. The physical examination revealed bilateral swelling of the lower extremities, while laboratory parameters showed increased levels of C-reactive protein, D-dimers and NT-pro BNP. Immediate transthoracic echocardiography (TTE) showed a left atrial mass measuring 60x27 mm, prolapsing across the mitral valve and causing valvular obstruction (fig 1 a-c). A computed tomography (CT) scan of the chest indicated a tumor mass within the left inferior pulmonary lobe with infiltration of the left pulmonary vein and a mass in the left atrium (LA). Magnetic resonance imaging (MRI) demonstrated a left atrial tumor prolapsing into the left ventricular cavity with protrusion to the right atrium through the atrial septal defect (fig 1d,e). Bronchial biopsy of the tumor mass exhibited an undifferentiated monomorphic blunt spindle cells with CD 99 positive expression which confirmed the diagnosis of metastatic monophasic synovial sarcoma. Due to a large tumor extension, cardiothoracic surgery was not indicated. The patient underwent chemotherapy with ifosfamide/doxorubicin.

Synovial sarcoma is a rare malignant mesenchymal neoplasm and represents 8-10% of all soft-tissue sarcoma (STS). It occurs mostly between 15 and 35 years of age, and more commonly in males. Although it has been observed to develop in the head, neck, lung, heart, mediastinum, and abdominal wall, it occurs predominantly in the soft tissues of the extremities. Overall 50% of patients develop metastatic disease at initial presentation. While hemoptysis, coughing, and chest pain are the usual symptoms, patients may not exhibit any of these, and synovial sarcoma may be discovered accidentally during a physical examination or imaging workup [1]. Left atrial masses encompass a diverse range of pathologies, including both neoplastic and non-neoplastic entities. Cardiac myxomas represent 50% of all benign cardiac tumors. To accurately diagnose the origin of left atrial masses, vari-

Received 06.03.2025 Accepted 08.05.2025
Med Ultrason
2025, Vol. 27, No 2, 240-241, DOI: 10.11152/mu-4511,
Corresponding author: Mijo Meter
Cardiovascular Diseases Department,
University Hospital of Split,
21000 Split, Croatia
E-mail: mijometer05@gmail.com
Phone: +385 / 98 975-2946

ous imaging techniques are employed, including echocardiography, CT and MRI [2].

Despite the fact that left atrial myxoma is the most prevalent benign cardiac tumor, in case of left atrial mass detected by echocardiography and history of previously known synovial sarcoma, we should also consider a possible cardiac metastasis. Multimodality imaging can be extremely important in those circumstances, not only for identifying the mass's features but also for determining the primary neoplasm's underlying site and potential cardiac involvement.

References

1. Corey RM, Swett K, Ward WG. Epidemiology and survivorship of soft tissue sarcomas in adults: A National Cancer Database report. Cancer Med 2014;3:1404-1415.
2. Tetera W, Wilk A, Król W, Braksator W. Asymptomatic Left Atrial Myxoma. J Cardiovasc Echogr 2022;32:116-118.

Intraneural ganglion cyst: an uncommon cause of foot drop

Po-Jia Pao, Yi-Hsiang Chiu, I-Chun Liu

Department of Physical Medicine and Rehabilitation, Cathay General Hospital, Taipei, Taiwan

To the Editor,

A 71-year-old man presented with two weeks of intermittent numbness in his left leg and weakness of the left ankle dorsiflexion. The numbness area ranged from the fibular head to the dorsum of the foot. He denied a history of prolonged left lateral decubitus position or recent trauma. His surgical history included pars repair due to L5/S1 spondylosis.

On physical examination, the muscle power of the left ankle dorsiflexion and eversion was 4, while ankle inversion was preserved. Steppage gait owing to the foot drop was noted when walking. Nerve conduction studies of the left peroneal nerve disclosed a conduction block between the above and below segments of the fibular neck. Additionally, a reduced amplitude of the sensory nerve action potential in the left superficial peroneal nerve was noted. These results implied left peroneal neuropathy across the fibular head. However, plain films demonstrated no spur or misalignment at the lateral component of the left femorotibial joint.

Further imaging studies were arranged to clarify etiology. Ultrasound revealed anechoic cystic lesions with posterior acoustic enhancement within the common peroneal nerve (fig 1A,B). No hypervascularity was noted around the lesion. Magnetic resonance imaging revealed multiple variably-sized, small cystic lesions at the anterolateral aspect of the fibula neck and mild edema in the anterior compartment muscle (fig 1C). No nerve root compression at the lumbosacral region was noted. Based on the findings, intraneural ganglion cysts at the left common peroneal nerve near the bifurcation were tentatively

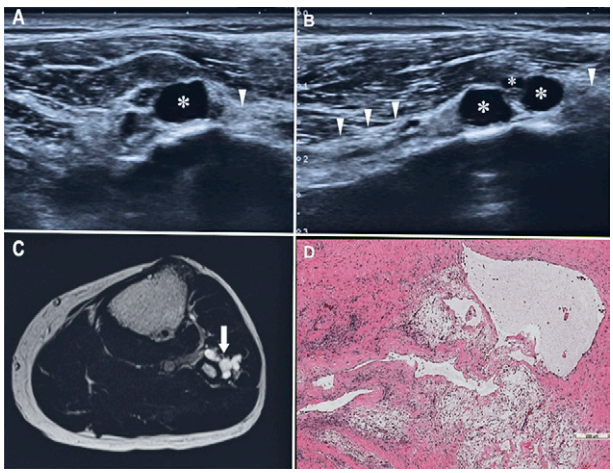

Fig 1. Ultrasound imaging at the level of the left fibular head in (A) a transverse view and (B) a longitudinal view revealed anechoic cystic lesions (asterisk) with posterior acoustic enhancement within the left common peroneal nerve (arrowhead). (C) Axial T2 weighted magnetic resonance imaging disclosed multiple variably sized, hyperintensity cystic lesions (arrow). (D) The specimen with a brown and elastic appearance, measuring 1.9x1.6x0.7 cm, was reported to be the ganglion cyst.

Received 08.02.2025 Accepted 23.02.2025
Med Ultrason
2025, Vol. 27, No 2, 241-242, DOI: 10.11152/mu-4512,
Corresponding author: I-Chun Liu, MD
Department of Physical Medicine and Rehabilitation, Cathay General Hospital
280 Renai Rd. Sec.4, 10630 Taipei, Taiwan
E-mail: jacy50521@gmail.com

impressed. Thus, surgical excision was performed, and the pathology report confirmed the diagnosis of ganglion cysts (fig 1D) At a follow-up one month after surgery, he reported significant improvement in numbness but only limited recovery of ankle dorsiflexion.

Intraneural ganglion cyst is a relatively uncommon type of extraarticular ganglia around the knee, commonly associated with the common peroneal nerve or its branches, leading to foot drop and paresthesia over the dorsum of the foot [1].

This case highlights the critical role of ultrasound as an effective first-line imaging modality. It provided real-time, non-invasive evaluation of a cystic lesion and its anatomical relationship with surrounding structures, guiding the decision to perform further imaging such as MRI to facilitate timely surgical decompression and excision [2].

References

1. Perdikakis E, Skiadas V. MRI characteristics of cysts and "cyst-like" lesions in and around the knee: what the radiologist needs to know. Insights Imaging 2013;4:257-272.
2. Neto N, Nunnes P. Spectrum of MRI features of ganglion and synovial cysts. Insights Imaging 2016;7:179-186.

Recurrence of low-grade endometrial stromal sarcoma during pregnancy following fertility-sparing management

Minsheng Chen, Yifei Tan, Jin Wang

Department of Ultrasound, West China Second University Hospital, Key Laboratory of Birth Defects and Related Diseases of Women and Children, Sichuan University, Chengdu, China

To the Editor,

A 33-year-old woman (G1P0) was diagnosed with low-grade endometrial stromal sarcoma (LGESS) two years ago. Ultrasonography revealed a heterogeneous hypoechoic mass located in the uterine fundus, measuring 3.6×3.3×4.1 cm. The mass showed an indistinct boundary and an irregular hypoechoic area, accompanied by rich blood flow signal (fig 1a). Fertility-sparing surgery was performed.

Transvaginal ultrasonography at 8 weeks gestation revealed a slightly hyperechoic nodule measuring 3.1×0.4×0.6 cm in the cervical canal (fig 1b). The nodule had well-defined borders and was initially suspected to be a polyp. However, after resection, it was diagnosed as a recurrence of LGESS. The patient declined pregnancy termination. At 29 weeks, an irregularly shaped hypoechoic mass measuring 6.3x2.8x4.1 cm was observed in the myometrium at uterine fundus, with poorly defined borders (fig 1c). Blood flow signals were noted within and around the lesion (fig 1d). Microvascular flow imaging (MVFI) showed a higher vascular density within the lesion compared to the surrounding myometrium (fig 1e). The patient again declined termination. At 34^{+4} weeks gestation, a cesarean section, total hysterectomy, and bilateral salpingectomy were performed. Multiple masses were found, the largest being 7.3×5.1×3.0 cm at uterine fundus. The tumor did not involve the parametrial tissues or fallopian tubes. Immunohistochemistry revealed positivity for CD10 (fig 1f). Postoperative follow-up for one year showed no evidence of tumor recurrence. The neonate showed no significant abnormalities.

LGESS is a rare but relatively favorable prognostic sarcoma, with hysterectomy being the standard treatment. However, fertility-sparing treatment is also an option for younger women desiring fertility preservation, although this may increase the risk of recurrence [1]. We present the first case of recurrent LGESS during pregnancy following fertility-sparing surgery. Physiological changes and the alterations in uterine morphology during pregnancy may result in misdiagnosis of LGESS as a benign condition. In our case, the recurrent lesion initially presented as a well-defined, slightly hyperechoic nodule

Received 17.02.2025 Accepted 23.03.2025
Med Ultrason
2025, Vol. 27, No 2, 242-243, DOI: 10.11152/mu-4513,
Corresponding author: Jin Wang
Department of Ultrasound,
West China Second University Hospital,
20, Renmin Road South,
610041, Chengdu, China
E-mail: quyangjinwangfu@163.com

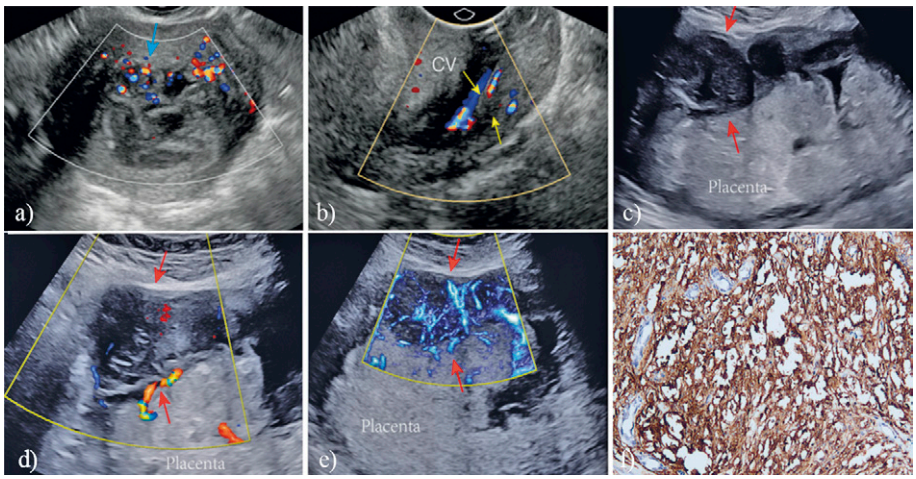

Fig 1. a) Ultrasonography of primary LGESS, showing a heterogeneous hypoechoic mass (blue arrow) with rich blood flow; b) recurrent LGESS, presenting as a slightly hyperechoic nodule (yellow arrow) in early pregnancy, and a hypoechoic mass (red arrows) in late pregnancy (c); Color Doppler ultrasound (d) and MVFI (e) indicate abundant blood flow; f) CD10 staining of the recurrent LGESS. scale bar 200 um.

on ultrasonography, lacking the typical characteristics of sarcoma. In late pregnancy, the lesion appeared as an irregular mass with rich blood supply, with MVFI providing helpful diagnostic support. Although no congenital abnormalities were found in the newborn, echoing a previous report [2], the potential impact of recurrent LGESS during pregnancy on fetal abnormalities requires further investigation.

References

1. Huang X, Peng P. Hormone Therapy Reduces Recurrence in Stage II-IV Uterine Low-Grade Endometrial Stromal Sarcomas: A Retrospective Cohort Study. Front Oncol 2022;12:922757.
2. Xie W, Cao D, Yang J, et al. Fertility-sparing surgery for patients with low-grade endometrial stromal sarcoma. Oncotarget 2017;8:10602-10608.

Analysis of a case with unilateral submandibular gland agenesis accompanied by ipsilateral sublingual gland cyst and calculi

Xiurong Wang[1], Yanan Li[2,3], Xin Li[3], Qingna Xiao[3], Qiaozhen Liu[3], Miao Shi[3]

[1]Department of Ultrasound, Jinan Zhangqiu District People's Hospital, Jinan, [2]School of Medical Imaging, Weifang Medical University, Weifang, [3]Department of Ultrasound, Liaocheng People's Hospital, Liaocheng, Shandong, China

Received 18.02.2025 Accepted 23.03.2025
Med Ultrason
2025, Vol. 27, No 2, 243-244, DOI: 10.11152/mu-4514,
Corresponding author: Miao Shi
Department of Ultrasound,
Liaocheng People's Hospital,
67 Dongchang West Road,
Dongchangfu District,
Liaocheng 252000,
Shandong, China
Phone: 0635-8272300
E-mail: shimiaoemail@163.com

To the Editor,

A 38-year-old male patient presented with a mass in the right sublingual area which appeared approximately 3 weeks before the presentation. Since its discovery, the patient had felt the mass gradually increasing in size. On physical examination, a mass approximately 1.5×1×1 cm was palpated in the right sublingual floor of the mouth. Ultrasound examination revealed a cystic mass in the right sublingual gland area with echogenic foci resem-

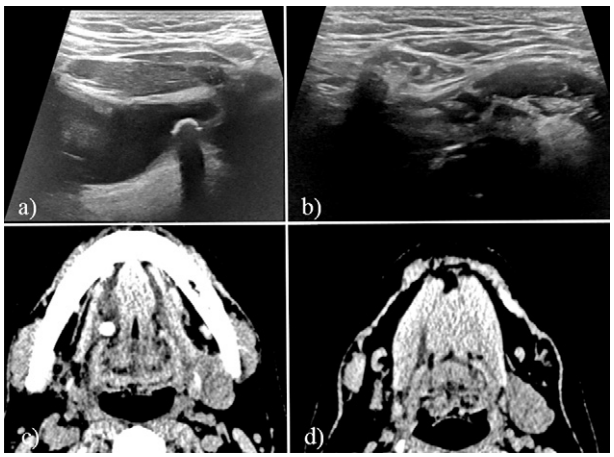

Fig 1. a) Anechoic area (3.5×2.6 cm) in right sublingual gland region containing hyperechoic focus (0.6×0.4 cm) with acoustic shadow; b) No gland tissue detected in right submandibular gland region; c) Nodular high-density image in right oral floor; d) Right submandibular gland poorly visualized.

bling calculi inside, and the right submandibular gland was not clearly visualized (fig 1a,b). The results of the computed tomography (CT) scan were similar (fig 1c,d). The intraoperative findings were consistent with ultrasound and CT diagnoses.

Salivary gland hypoplasia is a rare condition that rarely presents as an isolated lesion and is more commonly seen in the parotid glands [1]. The mechanism of salivary gland hypoplasia is not yet clear. Some studies speculate that it may be related to ectodermal defects of the first and second branchial arches, such as Treacher-Collins syndrome and orbital abnormalities [1,2]. However, no related developmental anomalies were found in this case. Osailan et al. found that after ligating the ducts of the submandibular glands in rats, the glands mostly atrophied [3]. After the ligation was released, the atrophied submandibular glands could regenerate and restore normal function. García-Consuegra et al. reported two cases of submandibular gland atrophy or aplasia related to calculi in the submandibular ducts, suggesting that obstructive sialolithiasis might be one of the causes of unilateral submandibular gland aplasia [2]. Some reports have shown that patients with submandibular gland hypoplasia may have compensatory hypertrophy of the sublingual glands, presenting as neck masses [1,4]. The mass in this patient may be a compensatory change in the sublingual gland.

Unilateral submandibular gland agenesis is relatively rare. Ultrasound is a convenient, non-invasive, and important method for diagnosing salivary gland agenesis.

References

1. Haktanir A. CT and MR findings of bilateral submandibular gland aplasia associated with hypertrophied symmetrical sublingual glands herniated through mylohyoid defects. Dentomaxillofac Radiol 2012;41:79-83.
2. García-Consuegra L, Rosado P, Gallego L, Junquera L. Unilateral absence of submandibular gland secondary to stones. Aplasia versus early atrophy. Med Oral Patol Oral Cir Bucal 2010;15:e752-754.
3. Osailan SM, Proctor GB, Carpenter GH, Paterson KL, McGurk M. Recovery of rat submandibular salivary gland function following removal of obstruction: a sialometrical and sialochemical study. Int J Exp Pathol 2006;87:411-423.
4. Srinivasan A, Moyer JS, Mukherji SK. Unilateral submandibular gland aplasia associated with ipsilateral sublingual gland hypertrophy. AJNR Am J Neuroradiol 2006;27: 2214-2216.

Left ventricular outflow tract obstruction due to subaortic pannus

Lin Ma[1], Xuejie Li[2]

[1]Department of Anesthesiology, Shenzhen Children's Hospital, [2]Department of Anesthesiology, West China Hospital, Sichuan University and The Research Units of West China, Chinese Academy of Medical Sciences, China

Received 07.03.2025 Accepted 23.03.2025
Med Ultrason
2025, Vol. 27, No 2, 244-245, DOI: 10.11152/mu-4515,
Corresponding author: Xuejie Li
Department of Anesthesiology,
West China Hospital, Sichuan University,
Chengdu, Sichuan Province, China
E-mail: lizuima@hotmail.com
Phone: +86-028-85423593

To the Editor,

We report the case of a 70-year-old male patient who was admitted with dyspnea and chest pain. The patient underwent mechanical aortic valve (19 mm St. Jude Medical Regent Valve) replacement for aortic stenosis sixteen years ago. Postoperative anticoagulation therapy was conducted using warfarin with the international normal-

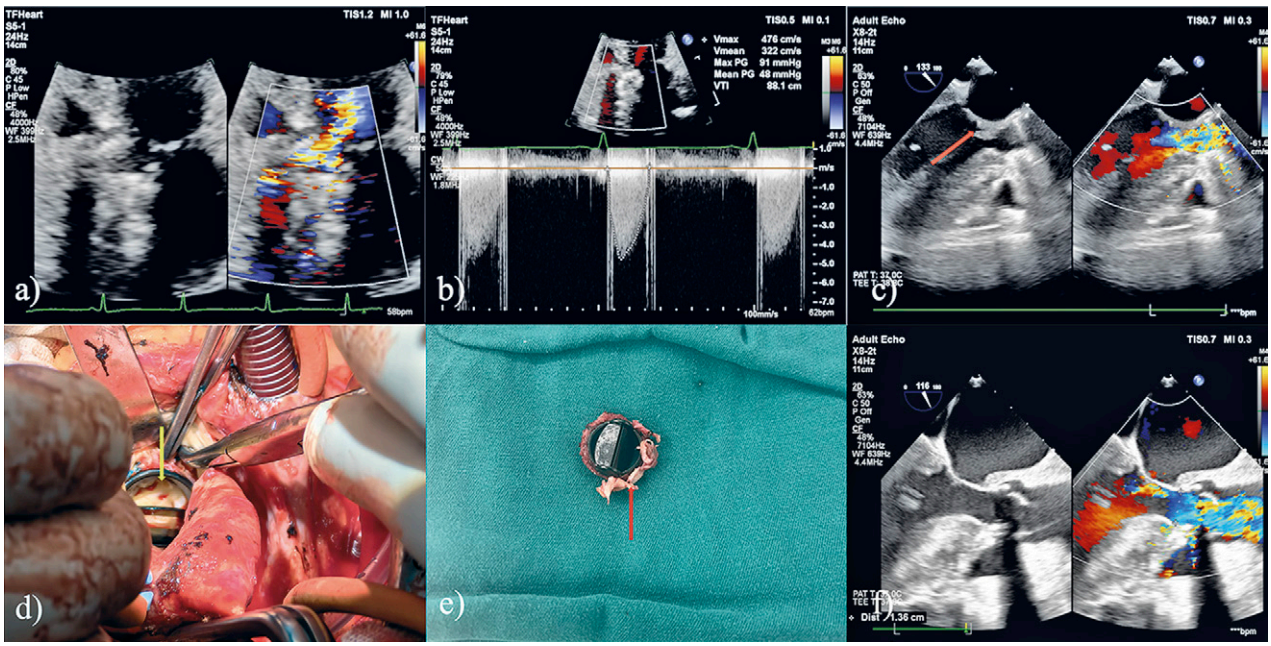

Fig 1. a) TTE showed severe aortic stenosis; b) TTE showed severe aortic stenosis with the peak pressure gradient increased to 91 mmHg; c) TEE examination revealed stenosis of the LVOT due to a membranous structure beneath the aortic valve; d) Intraoperative exploration revealed the structure of the subaortic pannus; e) The removed aortic mechanical valve shows the fibrous tissue beneath the valve (red arrow); f) LVOT obstruction disappeared after the aortic bioprosthetic valve was replaced. TTE, transthoracic echocardiography; LVOT, left ventricular outflow tract; TEE, transesophageal echocardiography.

ized ratio of 1.5-2.0. Antiplatelet drugs were not used. Transthoracic echocardiography showed severe aortic stenosis (fig 1a) with a peak velocity of 4.76 m/s and a mean gradient of 48 mmHg (fig 1b). The cause was speculated to be aortic mechanical valve dysfunction.

Considering the possibility of aortic mechanical valve dysfunction recurrence and the need for postoperative low-dose anticoagulation, aortic bioprosthetic valve replacement was scheduled. Intraoperative transesophageal echocardiography (TEE) examination revealed stenosis of the left ventricular outflow tract (LVOT) due to a membranous structure beneath the aortic valve (fig 1c). The patient underwent aortic bioprosthetic valve replacement through median thoracotomy under cardiopulmonary bypass. Intraoperative exploration revealed the structure of the subaortic pannus (fig 1d). The removed aortic mechanical valve shows the fibrous tissue beneath the valve (fig 1e). LVOT obstruction disappeared after the aortic bioprosthetic valve was replaced (fig 1f). The patient was discharged 9 days postoperative uneventfully.

Pannus formation is usually the cause of aortic mechanical prosthesis obstruction. Dysfunction of any mechanical prosthesis due to thrombus or pannus requires prompt diagnosis and therapy [1]. Repeat valve replacement is the only measure available for valve dysfunction due to pannus formation [2]. In the case of prosthetic aortic valve dysfunction caused by pannus, we should pay attention to whether the LVOT is obstructed by the subaortic pannus. In rare cases, the pannus extends to the left ventricular outflow tract, combined with stenosis of the left ventricular outflow tract. Intraoperative real-time TEE can be better identified.

References

1. Cianciulli TF, Saccheri MC, Lax JA, et al. Intermittent acute aortic regurgitation of a mechanical bileaflet aortic valve prosthesis: diagnosis and clinical implications. Eur J Echocardiogr 2009;10:446-449.
2. Kikuchi C, Ishihara S, Sugiyama Y, Ishii H. [Case report of a malfunctioning SJM 19 A aortic valve prosthesis requiring reoperation]. Kyobu Geka 2001;54:241-245.

Humerus-acromion angle model: a novel dynamic ultrasound technique for assessing shoulder mobility in adhesive capsulitis

Ke-Vin Chang[1,2,3], Wei-Ting Wu[1,2], Yi-Chung Shu[4], Che-Yu Lin[4], Levent Özçakar[5]

[1]Department of Physical Medicine and Rehabilitation and Community and Geriatric Research Center, National Taiwan University Hospital, Bei-Hu Branch, Taiwan, [2]Department of Physical Medicine and Rehabilitation, National Taiwan University College of Medicine, Taipei, Taiwan, [3]Center for Regional Anesthesia and Pain Medicine, Wang-Fang Hospital, Taipei Medical University, Taipei, Taiwan, [4]Institute of Applied Mechanics, College of Engineering, National Taiwan University, Taipei, Taiwan, [5]Department of Physical and Rehabilitation Medicine, Hacettepe University Medical School, Ankara, Turkey

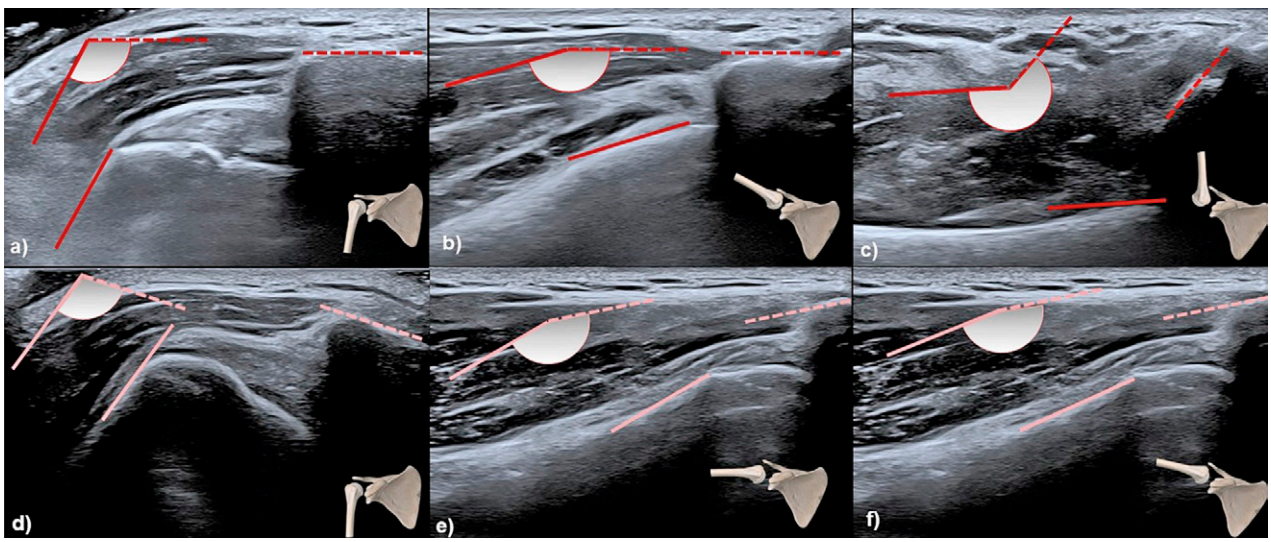

Fig 1. Snapshots of dynamic ultrasound imaging in a normal shoulder at neutral resting (a), abduction beyond 90 degrees (b), and full abduction to 180 degrees (c); and in adhesive capsulitis at neutral resting (d), abduction beyond 90 degrees (e), and maximal abduction (f).

To the Editor,

Dynamic ultrasound is a valuable tool for assessing shoulder movements and detecting early subacromial impingement syndrome [1]. A recently developed subacromial motion metrics model enables real-time visualization of the changes in the subacromial space through quantitative measurements (e.g. vertical acromiohumeral distance and humeral head rotating angle/radius) which have been integrated into a deep learning algorithm [2,3]. However, a key limitation of that model arises when the greater tubercle rotates beneath the lateral edge of the acromion, obstructing visualization. For avoiding this, the examiner must instruct the examinee to lower the arm once the greater tubercle is no longer visible. When acquiring relevant parameters, the humeral point aligned with the lateralmost edge of the acromion serves as a surrogate for the greater tubercle. This limitation introduces inaccuracies and fails to capture movement patterns in adhesive capsulitis, where humeral head rotation may be restricted at any degree of shoulder abduction, regardless of the greater tubercle's position relative to the lateral acromion.

Received 30.03.2025 Accepted 12.05.2025
Med Ultrason
2025, Vol. 27, No 2, 246-247, DOI: 10.11152/mu-4516,
Corresponding author: Ke-Vin Chang, MD, PhD
Department of Physical Medicine and Rehabilitation, National Taiwan University Hospital, Bei-Hu Branch and National Taiwan University College of Medicine, Taipei, Taiwan
E-mail: kvchang011@gmail.com

To address this issue, we propose the humerus-acromion angle model, which is based on the scapulohumeral rhythm during shoulder abduction. Scapulohumeral rhythm refers to the coordinated movements between the scapula and humerus during arm elevation [4], following roughly a 2:1 ratio. In other words, for every 3 degrees of shoulder abduction or flexion, the humerus moves 2 degrees at the glenohumeral joint while the scapula rotates 1 degree at the scapulothoracic joint. During routine shoulder ultrasound examination, placing the transducer along the acromion and instructing the participant to elevate the arm, reveals a progressive increase in the angle formed by the horizontal bony cortex of the acromion and the humeral contour distal to the greater tubercle (fig 1a-c, Video 1 on the journal site). The angle ranges from approximately 120° at the resting position to 240° at full abduction. This increase is not solely due to humeral head rotation against the glenoid but is also related to inferior migration of the humeral head.

In patients with frozen shoulder, as the arm is raised, this model demonstrates that the humerus-acromion angle ceases to increase despite continued shoulder abduction under passive examiner exertion (fig 1 d-f). Once the humerus-acromion angle reaches its limit, any further increase in abduction is attributed to scapular rotation which has a maximum range of roughly 60°. We believe this novel model more accurately identifies the contributing factors limiting full shoulder abduction in patients with glenohumeral adhesive capsulitis.

Acknowledgement: The present study was funded by National Taiwan University Hospital, Bei-Hu Branch (grant nos. 113-BH002 and 113-BH004), the Ministry of Science and Technology (grant nos. MOST 106-2314-B-002-180-MY3, 109-2314-B-002-114-MY3, 111-2314-B-002–161, NSTC 113-2314-B-002-208-MY2 and NSTC 114-2923-B-002-002-MY3), and Taiwan Society of Ultrasound in Medicine.

References

1. Wu WT, Lin CY, Shu YC, Chen LR, Özçakar L, Chang KV. Subacromial motion metrics in painful shoulder impingement: A dynamic quantitative ultrasonography analysis. Arch Phys Med Rehabil 2023;104:260-269.
2. Lin CY, Chou CC, Chen LR, et al. Quantitative analysis of dynamic subacromial ultrasonography: Reliability and influencing factors. Front Bioeng Biotechnol 2022; 10:830508.
3. Shu YC, Lo YC, Chiu HC, et al. Deep learning algorithm for predicting subacromial motion trajectory: Dynamic shoulder ultrasound analysis. Ultrasonics 2023;134:107057.
4. Scibek JS, Carcia CR. Assessment of scapulohumeral rhythm for scapular plane shoulder elevation using a modified digital inclinometer. World J Orthop 2012;3: 87-94.

An interesting mass: a case of retroperitoneal immature teratoma in a neonate

Xiaoli Ji, Huanhuan Ding, Xiang Zhang, Chunchun Jin

Department of Ultrasonography, The Wenzhou Third Clinical Institute Affiliated to Wenzhou Medical University, The Third Affiliated Hospital of Shanghai University, Wenzhou People's Hospital, Wenzhou, Zhejiang, China

To the Editor,

A 17-hour-old male neonate, born to a healthy 26-year-old primigravida, was hospitalized due to an abdominal mass. The pregnancy and delivery were uneventful, and the mother had no significant medical history. Physical examination revealed a firm, non-tender mass occupying the left abdomen. Laboratory results showed markedly elevated alpha-fetoprotein (AFP) at 165,241 ng/L. Ultrasound revealed a mixed cystic-solid mass (10×10 cm) in the left abdomen, with a relatively clear border, poor sound transmission in the cystic portion, uneven echogenicity and calcifications in the solid component, and accessible blood flow signal, suggestive of a retroperitoneal teratoma (fig 1a,b). Contrast-enhanced computed to-

Received 19.12.2024 Accepted 03.02.2025
Med Ultrason
2025, Vol. 27, No 2, 247-248, DOI: 10.11152/mu-4517,
Corresponding author: Xiaoli Ji
Department of Ultrasonography, Wenzhou People's Hospital, No. 299 Gu'an Rd, Wenzhou, Zhejiang 325000, China
E-mail: jix15140@gmail.com

mography (CT) showed a mixed density tumor (9.9×6.3 cm) in the retroperitoneal with soft tissue nodules and calcifications (fig 1d). Prenatal ultrasounds at 36 and 38 weeks had identified localized intestinal dilation, which was mistakenly interpreted as a bowel anomaly due to the fetal position and resolution of image (fig 1c). Four days after birth, the infant underwent surgical resection of an 11×9.5×7.5 cm cystic-solid mass. Histopathological analysis confirmed an immature teratoma, grade 3, located in the left retroperitoneum. Immunohistochemical staining was positive for CD10, CK, CK7, EMA, GFAP, Glypican-3, Hep, NSE, PAX-8, SALL4, and Vim, and showed a high Ki-67 index (90%). Negative markers included CD30, ER, OCT3/4, and PR.

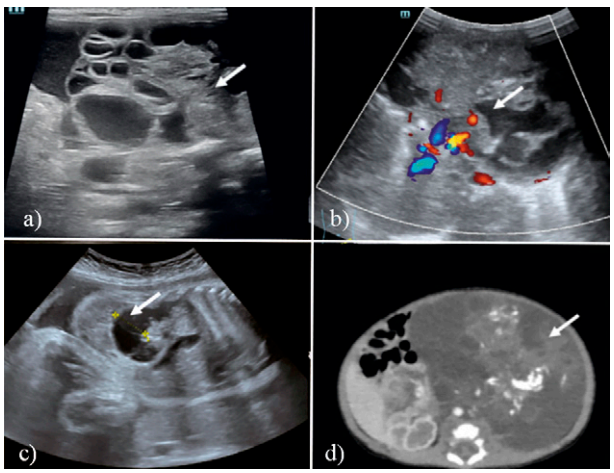

Fig 1. a) and b) Ultrasound revealed a mixed cystic-solid mass in the left abdomen, with a relatively clear border, poor sound transmission in the cystic portion, uneven echogenicity and calcifications in the solid component, and accessible blood flow signal; c) Prenatal ultrasound at 36 weeks; d) Contrast-enhanced CT showed a mixed density tumor in the retroperitoneal with soft tissue nodules and calcifications. The solid components of the lesion demonstrated mild to moderate enhancement following contrast administration, while the cystic regions showed no significant enhancement.

Fetal teratomas are most commonly found in the sacrococcygeal region, while retroperitoneal immature teratomas are extremely rare [1]. Immature teratomas are characterized by the presence of immature tissue derived from all three germ layers, with neuroectodermal components being a hallmark of immaturity [2]. AFP, a key marker in neonates, is elevated at birth and declines over time; elevated AFP levels serve as a critical biomarker for diagnosis and monitoring [3].

On ultrasound, these tumors often appear as mixed solid and cystic masses with ill-defined borders, calcifications, and rich blood flow. Prenatal ultrasound often struggles to diagnose retroperitoneal tumors due to fetal positioning and maternal factors such as obesity, leading to misinterpretation. Fortunately, early postnatal imaging and surgical resection minimized the risk of disease progression. Postoperatively, the infant recovered well, and AFP levels declined to normal ranges. Follow-up imaging at 1 year showed no recurrence.

References

1. Mahmood U, Talat N, Aziz MU, Mirza MB, Tahir W, Asif S. An atypical abdominal manifestation of retroperitoneal teratoma: Case report. Int J Surg Case Rep 2024;125: 110605.
2. Kürner K, Greuter L, Roethlisberger M, et al. Pediatric sellar teratoma - Case report and review of the literature. Childs Nerv Syst 2024;40:1259-1270.
3. Seyoum EA, Anderson LR. The case of the silent abdominal mass and elevated α-fetoprotein level in an infant. Pediatr Rev 2022;43:651-654.

A case of sternal metastasis caused by renal clear cell carcinoma

Zhe Wang, Chengfang Yu, Yilan Piao

Department of Medical Ultrasound, Yanbian University Hospital, Yanji, Jilin, China

Received 20.03.2025 Accepted 08.05.2025
Med Ultrason
2025, Vol. 27, No 2, 248-249, DOI: 10.11152/mu-4518,
Corresponding author: Yilan Piao
Department of Medical Ultrasound,
Yanbian University Hospital
1327 Juzi St. Yanji 133000, China
E-mail: 1419299989@qq.com

To the Editor,

A 71-year-old female patient was admitted with the chief complaint of “recurrent metastasis of right renal cancer for 6 months after 5 years of surgery”. Physical examination revealed a 5x5 cm mass in the lower part of the neck in the anterior chest, which was hard and

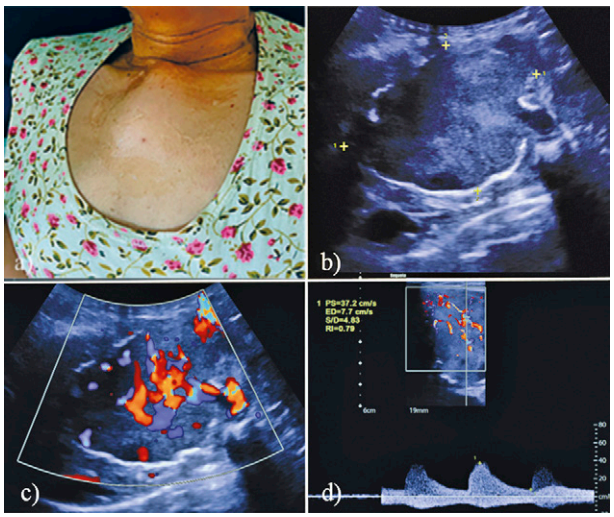

Fig 1. a) Physical examination shows a large mass in the anterior thoracic region of the neck; b) Ultrasound shows a large mass with mixed echogenicity anterior to the sternum; c) Abundant blood flow within the mass; d) spectral Doppler show speckled and striated blood flow signal in soft tissue, RI 0.79.

had poor mobility. Ultrasound examination showed a subcutaneous hypoechoic mass anterior to the sternum, measuring 6.1x4.29 cm, with poorly defined border, no distinct periphery, uneven internal echogenicity, edges as streaks of strong echogenicity, and sternal boundaries were not clear (fig 1). Using color Doppler ultrasound, rich blood flow signal was seen in the lesion. Ultrasound guided biopsy was performed, and pathology/immunohistochemistry results indicated that the mass represents renal clear cell carcinoma metastasis.

Renal clear cell carcinoma is the most common subtype of renal malignancy, and the most common site of metastasis is the lungs (70%), followed by lymph nodes (45%) and bones (32%) [1]. Primary and metastatic malignant tumors of the sternum are uncommon [2] and are clinically characterized by indurated protuberance and fullness of form, which in this case is consistent with previous literature [3]. Metastatic bone from renal clear cell carcinoma is a vascularized soft tissue replacement process [4]. The ultrasonographic aspect of malignant bone tumors is usually a mixed echogenic mass formed around the involved bone without a distinct envelope, within which punctate and striated blood flow signals are seen [5], which is consistent with previous literature descriptions. When a patient has a soft tissue mass in the anterior chest and neck, and ultrasound shows osteolytic changes, the possibility of sternal metastasis of malignant tumors should be considered in conjunction with the patient's medical history.

References

1. Cesana B, Cochet C, Filhol O. New players in the landscape of renal cell carcinoma bone metastasis and therapeutic opportunities. Int J Cancer 2025;156:475-487.
2. Carbognani P, Vagliasindi A, Costa P, et al. Surgical treatment of primary and metastatic sternal tumours. J Cardiovasc Surg (Torino) 2001;42:411-414.
3. Pyle JW, Ash JL, Hussain SM, Reid N, Anderson RC. Sternal resection and reconstruction after renal cell carcinoma metastatic to the sternum. J Thorac Cardiovasc Surg 2005;129:1177-1178.
4. Lee KS, De Smet AA, Liu G, Staab MJ. High resolution ultrasound features of prostatic rib metastasis: a prospective feasibility study with implication in the high-risk prostate cancer patient. Urol Oncol 2014;32:24.e7-11.
5. Madej T, Flak-Nurzyńska J, Dutkiewicz E, Ciechomska A, Kowalczyk J, Wieczorek AP. Ultrasound image of malignant bone tumors in children. An analysis of nine patients diagnosed in 2011-2016. J Ultrason 2018;18:103-111.

In vitro fertilization-embryo transfer (IVF-ET) combined with rectal clear cell carcinoma based on endometriosis: a case report

Shuang Zheng*[1], Xiaozheng Zhang*[1], Dawei Wang[2], Lin Li[1], Dongping Zheng[1]

** the authors share the first authorship*

[1]Department of Ultrasound, Renmin Hospital, [2]Department of Ultrasound, Taihe Hospital, Hubei University of Medicine, Shiyan, China

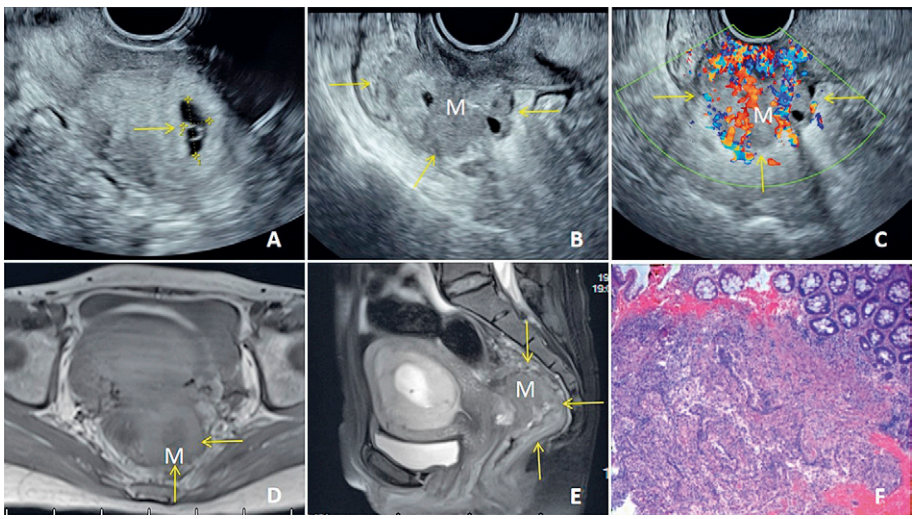

Fig 1. A. Ultrasound revealed a gestational sac (arrow) within the uterine cavity, clearly demonstrating the presence of an embryo and a yolk sac; B. Ultrasound revealed a hypoechoic mass (arrows) located behind the cervix, with irregular shape and uneven internal echo, and indistinct boundaries between the mass and both the cervix and the adjacent intestinal wall; C. Color Doppler ultrasound demonstrated abundant blood flow signals in the mass (arrows); D. Axial T1WI showed significant thickening of the mid-to-lower rectal wall accompanied by an irregular mass that appeared as a slightly hyperintense signal (arrows); E. Saggital T2WI illustrated the mass involved the entire circumference of the rectal wall, invaded the posterior wall of the cervix, and exhibited an isointense signal; F. The HE staining suggested that it might be clear cell carcinoma originating from endometriosis. M: mass.

To the Editor,

A 32-year-old woman, G1P0, was admitted due to lower abdominal pain persisting for 3 days, following the transfer of two embryos through in vitro fertilization-embryo transfer (IVF-ET) 22 days ago. The patient usually had regular menstruation and dysmenorrhea. Over the past four months, she had undergone multiple physical examinations due to abdominal distension, but no abnormal findings were observed.

The ultrasound examination revealed an early intrauterine pregnancy (fig 1A) and a solid mass located behind the cervix with irregular shape and heterogeneous internal echo (fig 1B). This mass was closely related to the rectum and cervix. Color Doppler ultrasound showed abundant blood flow signals in the mass, suggesting the possibility of a malignant mass (fig 1C). MRI showed significant thickening of the rectal wall in the middle to lower segment, accompanied by an irregular mass (fig 1D). The mass involved the entire circumference of the rectal wall and invaded the posterior wall of the cervix (fig 1E). It was considered rectal cancer, stage T4N2, with MRF(+) and EMVI (+).

Received 01.12.2024 Accepted 03.02.2025
Med Ultrason
2025, Vol. 27, No 2, 250-251, DOI: 10.11152/mu-4519,
Corresponding author: Dongping Zheng MD
Department of Ultrasound,
Renmin Hospital,
Hubei University of Medicine,
Shiyan 442000,
Hubei, China
E-mail: 59497066@qq.com

After obtaining the informed consent of the patient, a histopathological biopsy of the mass was performed through the rectum. A possible diagnosis of clear cell carcinoma originating from endometriosis was considered (fig 1F). The patient was informed of the relevant diagnosis and treatment plan, and chose to terminate the pregnancy, proceed with the removal of the mass, and undergo subsequent related treatments.

Endometriosis (EMs) is one of the common gynecological diseases [1]. Although it is considered as a benign disease, endometriosis has malignant biological behaviors, such as metastasis, invasion, and recurrence [2]. Studies have shown that endometriosis indeed has the potential to turn into clear cell carcinoma [3], and approximately 80% of these cases occur in the ovaries. It is extremely rare for endometriosis to metastasize to the rectum and transform clear cell carcinoma during pregnancy after IVF-ET like in our case. Furthermore, the existence of a correlation between IVF-ET and malignant transformation remains unknown.

Acknowledgments: The work was supported by Shiyan Science and Technology Bureau of Hubei Province (No. 22Y60)

References

1. Tan J, Xu T, Gou Y, et al. CCL20/CCR6 axis mediates macrophages to promote proliferation and migration of ESCs by blocking autophagic flux in endometriosis. Stem Cell Res Ther 2022;13:294.
2. Jin X, Feng J, Cheng X. LncRNA IGF2-AS promotes endometriosis progression through targeting miR-370-3p/IGF2 axis and activating PI3K/AKT/mTOR signaling pathway. J Assist Reprod Genet 2022;39:2699-2710.
3. Kvaskoff M, Mahamat-Saleh Y, Farland L V, et al. Endometriosis and cancer: a systematic review and meta-analysis. Hum Reprod Update 2021;27:393-420.

A rare case of concurrent fallopian tube cancer and ovarian cancer diagnosed via ultrasound imaging

Xiaoxue Wang*, Linhua Xuan*, Xu Guo, Guangming Jin

** the authors share the first authorship*

Department of Medical Ultrasound, Yanbian University Hospital, Yanji, Jilin, China

To the Editor,

A 62-year-old female patient was admitted to the Department of Gynecology with a chief complaint of a pelvic mass detected during physical examination 14 days prior. Upon specialist evaluation, no significant abnormalities were noted in the vulva and uterus. A palpable mass measuring approximately 11x12 cm was identified in the right adnexal region, characterized by moderate consistency and good mobility, while no abnormal findings were observed in the left adnexal area. Three-dimensional color Doppler ultrasound revealed that the uterus was positioned anteriorly, exhibiting a clear outline and normal morphology, with evidence of uterine atrophy, uniform echogenicity of the myometrium, and a linear endometrium. On the right side of the uterus, there was a cystic lesion measuring 97x96x98 mm (fig 1a), irregularly shaped with thick walls and multiple septations; some areas appeared anechoic while others contained hypoechoic foci resembling ovarian tissue (fig 1b). Ultrasound confirmed a cystic mass on the right side of the uterus. Serum CA125 levels were measured at 10.65 u/ml and CEA levels at 0.94 ng/ml. Under general anesthesia, transabdominal hysterectomy along with bilateral salpingo-oophorectomy and omentectomy were performed. During this procedure, a tubular mass of approximately 11 cm in length was excised, alongside an ovarian-like structure at its tip (fig 1c). Postoperative pathological analysis confirmed poorly differentiated ad-

Received 12.11.2024 Accepted 12.12.2024
Med Ultrason
2025, Vol. 27, No 2, 251-252, DOI: 10.11152/mu-4520,
Corresponding author: Guangming Jin
Department of Medical Ultrasound,
Yanbian University Hospital,
#1327 Juzi St.
Yanji 133000, China
Phone: +86-433-2660056
E-mail: jgm920@sina.com

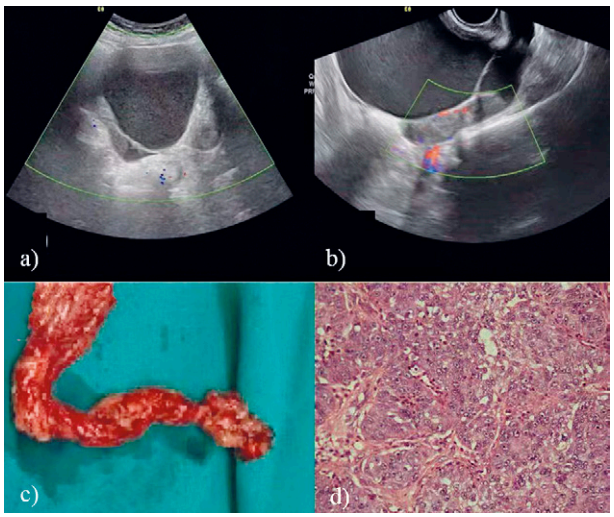

Fig 1. a) An anechoic region measuring 97x96x98 mm was identified on the right side of the uterus; b) The anechoic structure exhibited irregular contours, with thickened walls; additionally, some areas within this anechoic region contained hypoechoic foci that displayed echoes reminiscent of ovarian tissue; c) A tubular mass approximately 11 cm in length, featuring an ovarian-like component at its apex, was surgically excised; d) Postoperative pathological examination confirmed a diagnosis of poorly differentiated adenocarcinoma of the right fallopian tube and serous cystadenocarcinoma of the right ovary.

enocarcinoma of the right fallopian tube as well as serous cystadenocarcinoma of the right ovary (fig 1d).

Fallopian tube cancer is a rare malignant neoplasm of the female reproductive system, accounting for merely 0.5% of gynecological malignancies. It predominantly affects postmenopausal women, particularly those aged between 40 and 65 years. The early diagnosis of this condition poses significant challenges, resulting in a poor prognosis; the five-year survival rate ranges from approximately 21% to 44% [1]. Symptoms and signs associated with this disease are often atypical, leading to frequent oversight and delays in diagnosis. Clinically, it typically presents as vaginal discharge, abdominal pain, and pelvic mass – collectively referred to as the 'triad' of fallopian tube cancer. Prognosis varies significantly across different stages of fallopian tube cancer; thus, early detection and intervention can effectively manage disease progression. Ultrasound imaging can assess the location, size, characteristics of the mass, as well as any accompanying ascites. Computed tomography and magnetic resonance imaging provide clearer images than ultrasound and offer greater utility for staging purposes along with evaluating retroperitoneal lymph node enlargement and treatment planning. In this case study, the patient was diagnosed with concurrent fallopian tube cancer alongside ipsilateral ovarian cancer - a rare clinical occurrence. However, ultrasound alone cannot ascertain which tumor is primary; further evaluation through intraoperative findings combined with pathological results is necessary.

Acknowledgement: This work was funded by Natural Science Foundation of Jilin Province (YDZJ202201 ZYTS204).

Reference

1. Shalini B, Shalini R, Sameer G. Primary fallopian tube carcinoma: Preoperative diagnostic dilemma. Indian Journal of Health Sciences and Biomedical Research, 2023;16: 324-326.